be able to comfortably maintain the cytosolic Ca^{2+} in ROS at submillimolar concentrations.

Registry No. Na, 7440-23-5; Ca, 7440-70-2.

References

Bauer, P. J. (1988) *J. Physiol. (London) 401*, 309–327.
Cervetto, L., Lagnado, L., Perry, R. J., Robinson, D. W., & McNaughton, P. A. (1989) *Nature 337*, 740–743.
Cheon, J., & Reeves, J. P. (1988) *J. Biol. Chem. 263*, 2309–2315.
Cook, N. J., & Kaupp, U. B. (1988) *J. Biol. Chem. 263*, 11382–11388.
Cook, N. J., Zeilinger, C., Koch, K.-W., & Kaupp, U. B. (1986) *J. Biol. Chem. 261*, 17033–17039.
Cook, N. J., Molday, L. L., Reid, D., Kaupp, U. B., & Molday, R. S. (1989) *J. Biol. Chem. 264*, 6996–6999.
Fesenko, E. E., Kolesnikov, S. S., & Lyubarsky, A. L. (1985) *Nature 313*, 310–313.
Hagins, W. A., Penn, R. D., & Yoshikami, S. (1970) *Biophys. J. 10*, 380–412.
Hicks, D., & Molday, R. S. (1985) *Invest. Ophthalmol. Visual Sci. 26*, 1002–1013.
Hicks, D., & Molday, R. S. (1986) *Exp Eye Res. 42*, 55–71.
Hodgkin, A. L., McNaughton, P. A., & Nunn, B. J. (1985) *J. Physiol. (London) 358*, 447–468.
Lagnado, L., Cervetto, L., & McNaughton, P. A. (1988) *Proc. Natl. Acad. Sci. U.S.A. 85*, 4548–4552.
MacKenzie, D., & Molday, R. S. (1982) *J. Biol. Chem. 257*, 7100–7105.
Molday, L. L., & Molday, R. S. (1987a) *Biochim. Biophys. Acta 897*, 335–340.
Molday, R. S., & Molday, L. L. (1987b) *J. Cell Biol. 105*, 2589–2601.
Nakatani, K., & Yau, K.-W. (1989) *J. Physiol. (London) 409*, 525–548.
Nicoll, D. A., & Applebury, M. L. (1988) *Biophys. J. 53*, 389a.
O'Brien, P. J. (1976) *Exp. Eye Res. 23*, 127–137.
Schnetkamp, P. P. M. (1986) *J. Physiol. (London) 373*, 25–45.
Schnetkamp, P. P. M., & Bownds, M. D. (1987) *J. Gen. Physiol. 89*, 481–500.
Schnetkamp, P. P. M., Daemen, F. J. M., & Bonting, S. L. (1977) *Biochim. Biophys. Acta 468*, 259–270.
Schröder, W. H., & Fain, G. L. (1984) *Nature 309*, 268–270.
Sillman, A. J., Ito, H., & Tomita, T. (1969) *Vision Res. 9*, 1443–1451.
Uehara, F., Sameshima, M., Muramatsu, T., & Ohba, N. (1983) *Exp. Eye Res. 36*, 113–123.
Wong, S., & Molday, R. S. (1986) *Biochemistry 25*, 6294–6300.
Yau, K.-W., & Nakatani, K. (1984) *Nature 311*, 661–663.
Yau, K.-W., & Nakatani, K. (1985) *Nature 617*, 252–255.

Binding of Proteins to Specific Target Sites in Membranes Measured by Total Internal Reflection Fluorescence Microscopy†

Edwin Kalb, Jürgen Engel, and Lukas K. Tamm*

Department of Biophysical Chemistry, Biocenter, University of Basel, CH-4056 Basel, Switzerland

Received June 28, 1989

ABSTRACT: A new quantitative technique for measuring the binding of proteins to membranes is described. The method is based on a combination of total internal reflection fluorescence microscopy and the preparation of supported planar bilayers. Specific and reversible binding of a fluorescence-labeled monoclonal antibody to lipid haptens that were embedded in supported bilayers has been measured by this technique and compared to binding experiments that were conducted on membrane vesicles in solution. Equilibrium binding constants and kinetic parameters have been determined and used to expand the picture of the antibody–lipid hapten reaction. Estimates demonstrate that this technique is capable of measuring a broad range of binding constants (down to about 10^4 M^{-1}) using only small amounts of ligand and receptor.

An increasingly large number of cellular receptors have been identified for which quantitative thermodynamic and kinetic data on their interactions with ligands are highly desirable. Binding studies on whole cells by radioligand assays and related methods only yield semiquantitative data because of the usually high unspecific background binding and other complications (Klotz, 1982). Unspecific binding to the support and the undefined state of the receptor molecules affect solid-phase assays and other methods with solubilized receptors (Engel, 1984). In many cases, the functional reconstitution of receptors in synthetic lipid vesicles and other model membranes was successful (Klausner et al., 1984; Montal et al., 1981). However, the currently available methods for monitoring binding to membrane-bound receptors still suffer from a number of intrinsic and technical problems. Because of scattering problems, spectroscopic techniques in solution can usually be performed only with small sonicated vesicles at moderate concentrations. Some physical properties of such vesicles are quite distinct from those found in less curved membranes. Especially when large protein ligands with moderate binding constants are considered, it is often difficult to determine the amount of bound ligand in the presence of excess free ligand in solution. It is known that binding is often accompanied by an association of receptor molecules (Metzger et al., 1986; Schlessinger, 1988) and critically depends on the mobility of the receptors in the membrane (Axelrod, 1983). Multivalency of large ligands may also induce changes of the state of association and the receptor mobility. The latter parameters are determinable by microscopic techniques such

† This work was supported by the Swiss National Science Foundation Grants 3.039.87 (to J.E.) and 3.588.87 (to L.K.T.).

0006-2960/90/0429-1607$02.50/0

as fluorescence recovery after photobleaching [see, e.g., Jacobson et al. (1983) and Tamm (1988)] and total internal reflection fluorescence microscopy (Axelrod et al., 1984). Microscopic techniques offer the additional advantage that, if necessary, small regions of the membranes can be selected for observation whereas macroscopic techniques have to rely on the homogeneity of the system.

In the present work, we explored a new method that offers the advantages of microscopic observation and selective detection of bound ligand on membranes. Two recently introduced methods, namely, the preparation of supported planar bilayers (SPB)[1] and total internal reflection fluorescence microscopy (TIRFM), have been combined. SPBs are large continuous membranes which are supported on flat hydrophilic substrates, such as quartz microscope slides (Tamm & McConnell, 1985). They have been used recently to study the lateral diffusion of lipid-bound antibodies (Tamm 1988; Wright et al., 1988) and interactions between membrane-bound antigens and whole cells (Watts et al., 1984, 1986). TIRF can be used to excite selectively fluorescent molecules near a quartz–buffer interface (Hirschfeld, 1965; Harrick, 1967; Axelrod et al., 1984). Membrane-bound ligands reside in the thin layer which is excited by the evanescent wave of a totally internally reflected laser beam, but only a small portion of free ligands present in solution is illuminated. Since the fluorescence emission is proportional to the amount of bound fluorophore over a wide range of concentrations (Axelrod et al., 1984), this signal can be readily used to determine equilibrium binding and binding kinetics. Promising results have been obtained for the binding of insulin to its receptor by a similar approach (Sui et al., 1988). Also, the binding kinetics of an antigenic peptide to a class II histocompatibility antigen which was reconstituted in a supported bilayer have been measured (Sadegh-Nasseri & McConnell, 1989). However, in this case, unbound peptide was removed before the fluorescence intensities were measured by an epifluorescence technique.

In order to explore the method, a suitable test system was selected. Antibody–lipid hapten interactions were studied extensively in the past to follow immune reactions on membranes and to measure specific multivalent binding of large protein ligands to membranes [e.g., Kinsky and Nicoletti (1977), Balakrishnan et al. (1982), and Petrossian and Owicki (1984)]. Earlier, we have used a monoclonal anti-trinitrophenol (TNP) fluorescent-labeled IgG to study its binding to TNP-cap-eggPE which was embedded in small unilamellar vesicles at various mole fractions (Tamm & Bartoldus, 1988). This antibody–lipid hapten system is chemically well-defined, biophysically well characterized, and therefore, adequate to test the TIRFM method for studying binding of proteins to membranes. In the present work, we present a first systematic investigation of the specific binding of a large protein, i.e., the antibody, to a lipid hapten in a membrane by using this technique. We provide evidence for a reliable determination of equilibrium binding constants as well as for the measurement of association and dissociation kinetics.

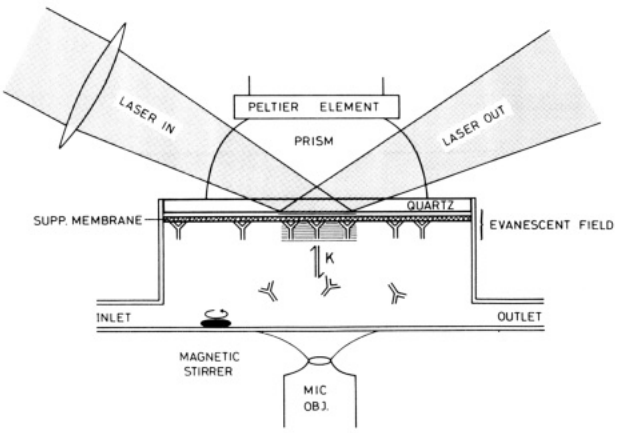

FIGURE 1: Experimental setup of the total internal reflection fluorescence microscopy sample cell used to measure antibody binding to supported planar bilayers (schematic drawing; not to scale). Two incoming laser beams (only one is shown) are directed through a quartz prism and totally internally reflected at the quartz–buffer interface of a quartz microscope slide. They form an interference pattern (8.0-μm periodicity) in an elliptical area at the interface. The region of the sample that is illuminated by the evanescent wave is marked with parallel lines. The sample cell which has a glass cover slip bottom is placed on an inverted microscope. The internal dimensions of the cell are 29.8 × 22.0 × 1.7 mm^3. A magnetic stirrer allows mixing of the cell contents during measurements, and a Peltier element is used to maintain constant temperature. The chemical equilibrium of antibodies free in solution and bound to the SPB is indicated by arrows.

Materials and Methods

Lipids and Antibody. DMPC, POPC, POPG, TNP-cap-eggPE, and Rh-DOPE (all from Avanti Polar Lipids) were pure on silica gel thin-layer chromatograms and were used without further purification. The monoclonal anti-TNP IgG (γ_{2b},κ) was harvested from cultures of the cell line GK14-1, purified, and labeled with fluorescein as described (Tamm, 1988). It had a high binding activity in ELISA tests, and 0.4–1.2 mol of fluorescein bound per mole of antibody (Tamm, 1988). N^{ϵ}-2,4-DNP-L-lysine was from Sigma.

Supported Planar Bilayers (SPBs). SPBs were prepared as described (Tamm, 1988). Quartz slides (4 × 2.5 cm^2) were used instead of silicon wafers. The quartz slides were boiled for 20 min in 10% Contrad 90 cleaning solution (Technosa, Lausanne, Switzerland), sonicated for 30 min in a bath sonicator, and rinsed extensively with destilled water. They were subsequently treated with dilute HF (1:50 with destilled water) for 1 min and extensively rinsed with destilled water (Tamm & McConnell, 1985). The quartz slides were further cleaned in a plasma cleaner (Harrick Scientific Corp.) under argon for 10 min immediately before the monolayers were transferred at 36 mN/m. The matrix lipid was DMPC. The different amounts of lipid hapten were present in the second monolayer trough and therefore were incorporated asymmetrically only in the outer monolayer of the SPB. This corresponds to the total amount of 20 pmol of hapten in the case of 1 mol % lipid hapten. The SPB was never exposed to air after preparation. The lateral diffusion coefficients of NBD-DMPE incorporated into SPBs on quartz slides were identical with those determined earlier on oxidized silicon wafers (Tamm, 1988).

Total Internal Reflection Fluorescence Microscopy (TIRFM). The quartz slide with the SPB was mounted onto a special sample cell which was made from PTFE Teflon and which had a glass cover slip bottom (Figure 1). The FRAP apparatus [described earlier by Tamm (1988)] was modified

[1] Abbreviations: DMPC, 1,2-dimyristoyl-3-*sn*-phosphatidylcholine; DNP, 2,4-dinitrophenol; ELISA, enzyme-linked immunosorbent assay; FRAP, fluorescence recovery after photobleaching; NA, numerical aperture; NBD-DMPE, *N*-(7-nitro-2,1,3-benzoxadiazol-4-yl)-1,2-dimyristoyl-3-*sn*-phosphatidylethanolamine; PIPES, piperazine-*N*,*N*′-bis(2-ethanesulfonic acid); POPC, 1-palmitoyl-2-oleoyl-3-*sn*-phosphatidylcholine; POPG, 1-palmitoyl-2-oleoyl-3-*sn*-phosphatidylglycerol; Rh-DOPE, *N*-(lissamine rhodamine B sulfonyl)-1,2-dioleoyl-*sn*-3-phosphatidylethanolamine; SPB, supported planar bilayer; TIRF, total internal reflection fluorimetry; TIRFM, total internal reflection fluorescence microscopy; TNP, 2,4,6-trinitrophenol; TNP-cap-eggPE, egg *N*-[[(2,4,6-trinitrophenyl)amino]caproyl]phosphatidylethanolamine.

for TIR illumination. The sample cell was placed onto the stage of the inverted fluorescence microscope (IM35, Zeiss, Oberkochen, FRG). After passage through the acoustooptic modulator, the argon ion laser beam was split by a 1:1 beam splitter. The two beams entered the quartz microscope slide through a hemicylindrical quartz prism at an angle of 72° to the normal (the critical angle for the quartz–buffer interface is 65.4°). The prism was fixed to the microscope, temperature-controlled by a Peltier element, and optically coupled to the slide with immersion oil. The sample could be scanned on the translation stage within an area of 1.5 × 0.3 cm^2. Both beams were focused and totally internally reflected on the same spot in the sample (see Figure 1), where an interference fringe pattern of 8.0-μm periodicity was produced (Weis et al., 1982). This pattern provided contrast in the sample and aided focusing the microscope. A 40× water immersion objective (NA = 0.75, Zeiss) was used to collect the emitted light. The fluorescence emission arising from the central part (about 4000 μm^2) of the total illuminated area passed through an image plane diaphragm and was collected by the photomultiplier tube. The photocurrent was A/D converted and directly fed into an extended memory (1 MByte) of the Apple IIe microcomputer. The microscope is easily switched from the TIR into the epiillumination (used for FRAP) mode by a single mirror change.

Typically, the fluorescence intensities of six to eight different spots were determined per sample point in equilibrium binding and dissociation kinetic experiments. Thirty to forty minutes was allowed for equilibration after each addition of antibody in the equilibrium binding experiments. All experiments were done at 25 °C with continuous stirring.

Calculation of the Ratio of the Fluorescence Intensity of Bound and Unbound Ligands. The ratio of the contribution of bound (I_b) and unbound (I_s) ligands to the total fluorescence intensity was calculated according to

$$I_b/I_s = c_b[\exp(-z/d)]/(c_s d) \quad (1)$$

where d is the $1/e$ penetration depth of the evanescent wave, z is the distance of the bound ligand from the interface, and c_b and c_s are the concentrations of the bound and unbound ligands (Harrick, 1967). In these calculations, z was taken to be 20 nm.

Large Unilamellar Vesicles. The appropriate amounts of lipids were mixed from stock solutions in $CHCl_3$ (5.0 mol % hapten, POPC/Rh-DOPE/TNP-cap-eggPE/POPG = 85/5/5/5 mol/mol; 1.0 mol % hapten, 85/5/1/9; 0 mol % hapten, 85/5/0/10 mol/mol). The solvent was removed by gentle flushing with N_2. PIPES (10 mM) buffer, pH 7.4, containing 0.15 M NaCl, and solid octyl β-D-glucoside were added to give final concentrations of 5 mM lipid and 75 mM octyl glucoside. The resulting solution was dialyzed for 2 days in a small home-built dialyzing cell with continuous buffer exchange (5 mL/h). The vesicle suspensions were fractionated by differential centrifugation at 4 °C. After 20 min of centrifugation at 22700g (5000 rpm/Ti50 rotor, Beckman Instruments) the supernatant was centrifuged again for 1 h at 104000g (23000 rpm/Ti50 rotor, Beckman Instruments) and the pellet was resuspended in 50% of the initial volume. This resulted in vesicles of a mean diameter of 200 nm as judged by electron microscopy after negative staining with uranyl formate. The phospholipid concentration was determined (Ames & Dubin, 1960) and was typically about 5 mM.

Vesicle Titrations. Binding experiments to vesicles were conducted by the resonance energy transfer technique as described (Tamm & Bartoldus, 1988). The binding parameter B is defined by $B = 1 - F/F_0$, where F_0 and F are the fluorescence intensities before and after vesicle additions, respectively.

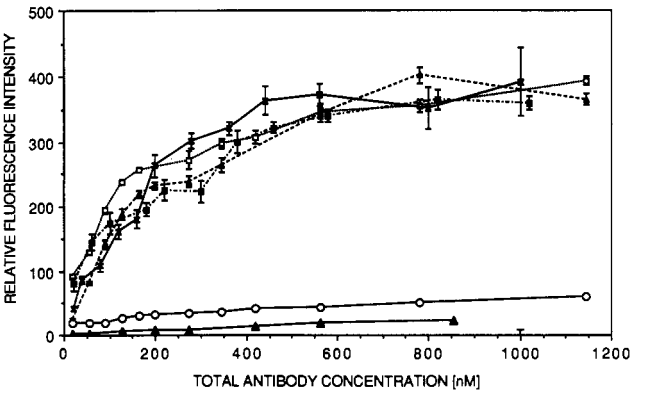

FIGURE 2: Binding of FITC-labeled antibody to supported planar bilayers (DMPC) containing the lipid hapten TNP-cap-eggPE. Four binding isotherms measured by TIRFM at 1.0 mol % hapten (×, △, □, ■) are shown. The data are normalized at the saturation intensity and plotted at the intensity of one typical experiment (the variation of the different saturation intensities is given in Table I). The error bars indicate the standard deviation of the six to eight different areas of the SPB measured per sample point. Unspecific binding to DMPC (○) and plain quartz (▲) are shown in the lower two curves. The theoretical background value from labeled molecules in solution (see Materials and Methods) at 1000 nM antibody is about 1% of the saturation intensity at 1 mol % lipid hapten (T).

Data Analysis. The experimental data of the binding isotherms were fit to the simple Langmuir binding model, $K_{app}c_A^f = c_A^b/[(c_H^0/2) - c_A^b]$, by using a Marquardt algorithm on a Vax 8830 computer. c_A^f and c_A^b are the concentrations of the free and bound antibody; c_H^0 is the total concentration of the lipid hapten in the membrane. The amount of total active antigen combining sites, i.e., the concentration of active antibody, was determined by a stoichiometric titration (Eisen & Siskind, 1964) with N^ϵ-2,4-DNP-L-lysine in the presence of excess antibody (0.38 mg/mL). This concentration was used in all calculations and was found to be 50% of the protein concentration as determined by Lowry et al. (1951) with BSA as a standard. The amount of total lipid hapten in the outer monolayer was taken to be 60% of the total lipid hapten in SUVs and 50% of the total lipid hapten in LUVs. The binding constants (K_{app}) that were obtained by this method are only apparent, since this simple model neglects effects due to the bivalency and the large size of the ligand [cf. Tamm and Bartoldus (1988)].

Results

Equilibrium binding of fluorescent labeled TNP-specific antibodies to TNP-cap-eggPE hapten in supported planar bilayers (SPBs) was measured by TIRFM. Figure 2 shows four representative individual binding curves which were obtained on SPBs, each containing 1 mol % of the lipid hapten TNP-cap-eggPE. Two control experiments showing the low level of nonspecific binding to a plain DMPC bilayer (i.e., in the absence of the specific lipid hapten) and to an uncoated quartz surface are also shown in Figure 2. The theoretical background intensity that is expected from the number of labeled but unbound IgG molecules in the volume illuminated by the evanescent wave is negligible (Figure 2; see also Table III). Standard deviations of data points collected from different areas of a single supported bilayer are typically within 1 and 3%. This illustrates the homogeneity of the SPBs.

Figure 3 demonstrates the effect of the binding site density on the binding isotherms. Binding was measured at 0.2, 1.0, and 5.0 mol % hapten, and the resulting isotherms are plotted after correction for nonspecific binding to plain DMPC

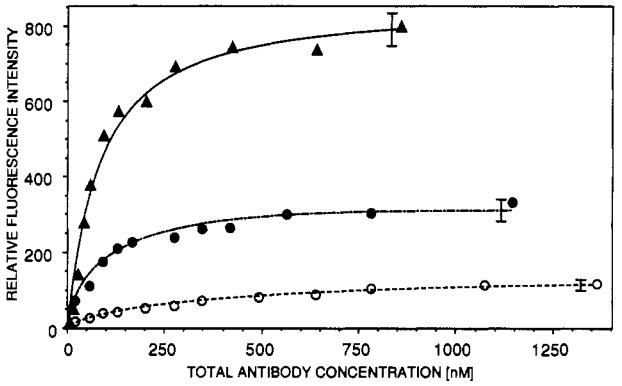

FIGURE 3: Background-corrected binding isotherms of FITC-labeled antibody to 0.2 (○), 1.0 (●), or 5.0 mol % (▲) lipid hapten in supported planar bilayers. The error bars indicate the uncertainty (±5%) in the fluorescence intensity at saturation, which was estimated from Figure 1. The lines represent the best fits of the data to simple Langmuir adsorption isotherms.

Table I: Apparent Binding Constants for Antibody Binding to Supported Planar Membranes (DMPC) Containing Various Mole Percentages of the Lipid Hapten TNP-cap-eggPE As Measured by TIRFM

lipid hapten density in the membrane (mol %)	total lipid concn (μM)	$K_{app} \times 10^{-7}$ (M^{-1})	rel fluorescence intensity at saturation
0.2	1.8	0.7	130
1.0	1.8	1.3	nd[a]
		1.0	250
		2.1	345
5.0	1.8	1.8	700
		4.6	840

[a] nd, not determined.

Table II: Apparent Antibody Binding Constants Obtained with Small Unilamellar (SUV) and Large Unilamellar Vesicles (LUV) and Determined by Resonance Energy Transfer

	SUV		LUV	
lipid hapten in membrane (mol %)	total antibody concn[a] (nM)	$K_{app} \times 10^{-7}$ (M^{-1})	total antibody concn[a] (nM)	$K_{app} \times 10^{-7}$ (M^{-1})
0.2	15.7	5.5		nd[b]
1.0	15.7	19 ± 9	5.0	(0.56)[c]
5.0	2.5	15 ± 10	5.0	2.9

[a] Total concentration of active antigen combining sites divided by 2 (see Materials and Methods). [b] nd, not determined. [c] Due to light scattering of the vesicle solution this value is only approximate.

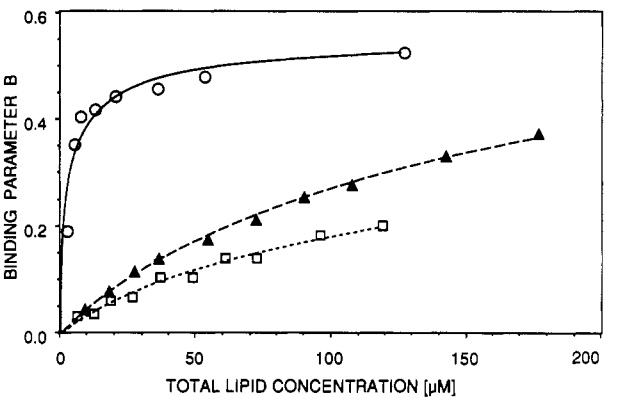

FIGURE 4: Binding of FITC-labeled antibody to LUVs as determined by resonance energy transfer. The binding parameter B is derived from the decrease of the fluorescence intensity at 513 nm. Data obtained for 5.0 (○), 1.0 (▲), and 0 mol % (□) lipid hapten are shown. The high amount of unspecific background (0 mol % hapten) is most likely due to light scattering.

membranes (see Figure 2). The relative fluorescence intensities near saturation increase with increasing lipid hapten concentrations, but this increase is not proportional to the increase of potential binding sites in the membrane (see Discussion). The error bars in Figure 3 indicate the standard deviations near saturation derived from the four independently measured but normalized binding curves at 1 mol % lipid hapten shown in Figure 2. The lines in Figure 3 represent the best fits of the data to a simple Langmuir adsorption binding model as described under Materials and Methods. The apparent binding constants which were obtained by these fits to the TIRFM binding data are summarized in Table I. Binding constants were in the range of 1×10^7 M^{-1}, and they were only slightly dependent on the lipid hapten density (Table I). As a control, the binding of the soluble hapten N^{ϵ}-2,4-DNP-L-lysine to our antibody was determined by tryptophan fluorescence quenching according to the method of Eisen and Siskind (1964) (data not shown). This resulted in a binding constant of $K = 5 \times 10^7$ M^{-1}. Note that the value for monovalent binding in solution was of the same order of magnitude as the apparent binding constants for binding to membranes for which simultaneous binding of the bivalent antibody to two lipid haptens is expected. The additional NO_2 group on TNP compared to DNP has no major effect on its affinity to this antibody, since we did not observe any difference in ELISAs to DNP- or TNP-bovine serum albumin (data not shown).

We have earlier measured the binding of this antibody to small unilamellar vesicles (SUV) with an average diameter of 30 nm (Tamm & Bartoldus, 1988). In order to compare these previous results to our present TIRFM binding curves, we reanalyzed some of the SUV binding curves with the Langmuir model with a fixed lipid hapten to antibody ratio (2:1) as was done with the SPB binding curves. These results are shown in Table II. The apparent binding constants obtained with the small vesicles were 10–20 times larger than those obtained for the planar supported bilayers (Table I).

In order to test whether this difference could be due to the high curvature of the vesicles, binding has been measured to large unilamellar vesicles (LUV) with a mean diameter of 200 nm. Two binding curves at 1 and 5 mol % lipid hapten and a control with no lipid hapten are shown in Figure 4. These data were obtained by a resonance energy transfer method in a fluorescence cuvette. The rather large background signal seen in the titration with vesicles containing no lipid hapten is most likely due to light scattering. Therefore, only the apparent binding constant at 5 mol % could be determined reliably ($K = 2.9 \times 10^7$ M^{-1}; see Table II). The binding constant for vesicles of 200-nm diameter was similar to the values obtained for planar bilayers, suggesting that binding is indeed facilitated by high membrane curvatures.

The time course of the association reaction could also be followed by TIRFM. Figure 5 shows that the association reaction depended on both the lipid hapten density in the membrane and the bulk antibody concentration. The lag period seen at the beginning of all association curves is probably due to a stirring gradient in the solution near the spatially fixed SPB.

The reversibility of the binding reaction to the planar membrane was confirmed by a competition experiment (Figure 6): A 3-fold excess of unlabeled antibody was added to a SPB which had been equilibrated with fluorescent antibody under nonsaturating conditions. After a short increase, the relative fluorescence intensity decreased to a plateau value after 4–5 h. Assuming complete reversibility, the calculated final

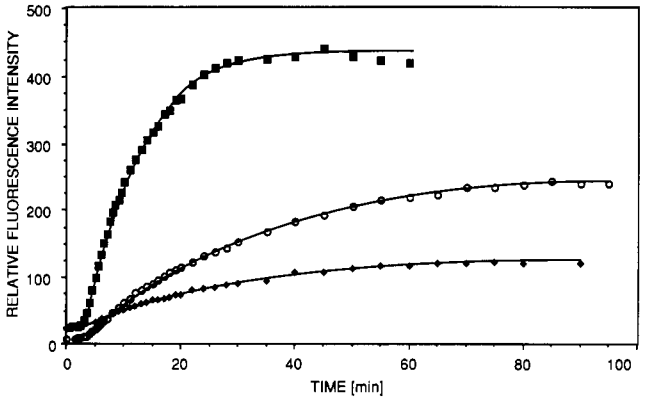

FIGURE 5: Association kinetics of FITC-labeled antibody to SPBs with incorporated lipid hapten measured by TIRFM. The increases of the relative fluorescence intensity at 1 mol % lipid hapten after addition of 150 nM (○) and 75 nM (♦) antibody and at 5 mol % hapten (■) after addition of 150 nM antibody are shown. A lag time of about 2 min was detected in all three experiments.

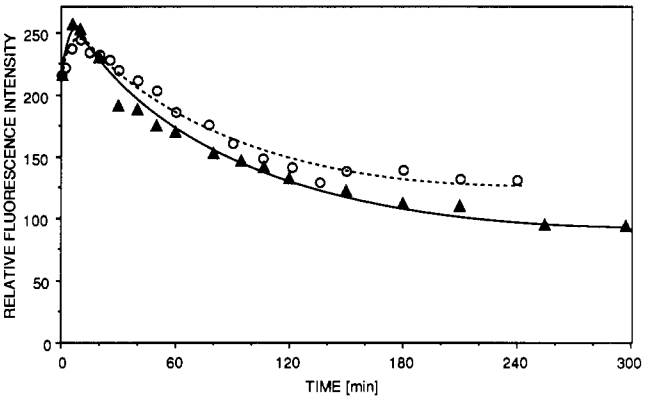

FIGURE 6: Competition experiments showing the reversibility of antibody binding to SPBs. At time zero unlabeled antibody (c = 450 nM) is added to a membrane containing 1.0% hapten which has been equilibrated with 150 nM FITC-labeled antibody. Assuming that 66% saturation has been reached at 150 nM antibody (see Figure 3) and that complete saturation is reached after equilibration with the unlabeled antibody, the end value is expected to be 38% of the initial fluorescence intensity. Two independent experiments are shown: one decreases to 43% (90% reversible) (▲) and the other to 60% (70% reversible) (○) of the initial fluorescence intensity. The characteristic time for an exponential decay, $\tau_{1/e}$, is about 120 min in both experiments.

fluorescence intensity should be 38% of the initial value under the employed experimental conditions. In two independent experiments (Figure 6) the signal decreased to about 43% (i.e., 90% reversibility) and to about 60% (i.e., 70% reversibility). When unlabeled antibody is added in excess, fast additional binding to still-unbound lipid haptens is expected. Part of this process is observable due to a fraction of labeled molecules in the mixture. This may explain the transient increase of the fluorescence intensity during the first 10 min (Figure 6).

In order to estimate the range of binding constants that can be measured by TIRFM in further applications, we have calculated the limiting concentrations for various receptor densities. The evanescent wave illuminates in addition to the membrane itself also a thin layer of solution adjacent to the membrane (see Figure 1). This background signal increases with increasing ligand concentration in solution. Therefore, the ratio of the contributions of bound (I_b) and unbound (I_s) ligands to the total fluorescence intensity depends on the receptor density, binding constant, and free ligand concentration. This is shown in Table III for several cases, where the ratio I_b/I_s has been calculated for various receptor densities and ligand concentrations assuming full saturation of the receptors.[2]

Table III: Estimate of Useful Concentration Ranges of the TIRFM Method[a]

		I_b/I_s		
	area/receptor (nm^2):	60	200	2000
c_{ligand} (M)	$c_{receptor}$ (pmol dm^{-2}):	270	83	8.3
10^{-3}		0.23	0.068	0.0068
10^{-4}		2.3	0.68	0.068
10^{-5}		23	6.8	0.68
10^{-6}		230	68	6.8

[a] The TIRFM signal ratios of bound (I_b) and unbound (I_s) ligands are tabulated at various receptor densities.

The second column of Table III corresponds to our antibody–lipid hapten system at greater than or equal to 2.3 mol % lipid hapten (area per antibody = 60 nm^2). The broken line in Table III indicates the limit at which the bound signal exceeds the solution signal. Useful titrations can, therefore, be conducted only in concentration ranges below this line.

Discussion

The present work describes a new method to measure binding of fluorescent ligands to specific target sites in membranes. Our results clearly demonstrate that a consistent set of kinetic and equilibrium binding data for the antibody–lipid hapten binding reaction can be obtained by TIRFM on supported planar bilayers. It is clear from Figures 2 and 3 that reproducible binding curves with a relatively low statistical noise can be obtained by this method. In contrast to many other popular techniques, these are true equilibrium binding isotherms, as demonstrated by the high reversibility shown in Figure 6. The high reversibility and the low unspecific binding obtained with SPBs contrast favorably with earlier binding experiments by TIRF to protein-coated surfaces in which high unspecific binding and low reversibility precluded a quantitative evaluation of specific binding (Kronick & Little, 1975; Thompson & Axelrod, 1983).

The affinity of the monoclonal antibody employed in the present study to its soluble hapten N^{ϵ}-2,4-DNP-L-lysine is moderately high. The binding constant of $K = 5 \times 10^7$ M^{-1} falls in the range of values (10^5–10^{10} M^{-1}) reported for other antibody–hapten interactions (Karush, 1978). These values determined for small haptens in solution may be interpreted as intrinsic binding constants of a single antigen combining site. Binding to membrane-associated lipid haptens implies complex mechanisms due to the possibility of multiple interaction of the bivalent antibody and due to size exclusion effects [e.g., Stankowski (1983) and Tamm and Bartoldus (1988)]. To facilitate comparison of data obtained by different methods, binding isotherms were analyzed by the simple Langmuir adsorption model and apparent binding constants of 10^7–10^8 M^{-1} were obtained. These overall constants for SPBs, large vesicles, and small vesicles, respectively, are much lower than expected on the basis of an intrinsic binding constant of 5×10^7 M^{-1} since bivalent antibodies can bind to more than one hapten at the lipid hapten densities employed (Tamm & Bartoldus, 1988). Therefore, we conclude that the binding to membrane-bound hapten sites is weakened by steric hinderance or by unfavorable interactions such as charge repulsion. These effects are apparently relaxed in part by higher exposure of the TNP group in more highly curved model

[2] For the calculation of I_b/I_s, we assumed that the bound fluorophores were at an average distance of 20 nm from the quartz buffer interface. The postulated aqueous layer between the supported bilayer and its support (Tamm & McConnell, 1985) is estimated to be 10 nm thick [cf. Schneider et al. (1986)]. The thickness of the bilayer is 4 nm, and an IgG molecule is about 12 nm long.

membranes (SUV). Alternatively, additional hydrophobic contacts of the antibody with the membrane may be possible in highly curved membranes, as has been noted before in studies of the interactions of amphiphilic peptides with model membranes (Kuchinka & Seelig, 1989; Tamm et al., 1989).

Only moderate changes of the apparent binding constants were observed upon changing the lipid hapten density in the range from 0.2 to 5 mol % lipid hapten (Table I). A dependency of the apparent binding constants on the binding site density is expected due to the bivalency of the antibody and size exclusion effects. This was indeed observed by Tamm and Bartoldus (1988) with SUV. In the present experiments with planar membranes, we expected an even clearer manifestation of this effect, since here the protein is titrated instead of the lipid hapten. Nevertheless, our present apparent binding constants appear to be more weakly dependent on the lipid hapten density than those measured with SUV (see Tables I and II). Further experiments will be needed to substantiate this dependence and correlate the results with binding models including large ligand effects and the effect of multiple binding sites.

Although it is difficult to compare fluorescence intensities between different experiments, the ratios of the fluorescence intensities at saturation can give an estimate of the amount of bound antibody. The ratio of the fluorescence intensities at antibody saturation between 5 and 1 mol % lipid hapten has been calculated from Table I and is between 2.0 and 3.5. This corresponds very well to theoretical considerations in which each antibody covers an area of about 60 nm^2 (Tamm & Bartoldus, 1988; Coleman et al., 1976) on the membrane and thus full saturation of the membrane will be achieved at 2.3 mol % lipid hapten in the membrane [area per lipid = 70 Å^2 (White & King, 1985)]. Therefore, the ratio of the fluorescence intensity at saturation with 5 mol % lipid hapten to the fluorescence intensity at saturation with 1 mol % lipid hapten cannot exceed 2.3.

In addition to the measurement of equilibrium binding, we also explored the possibility of obtaining kinetic data by TIRFM. Figures 5 and 6 demonstrate that this technique can measure association and dissociation kinetics. The most simple description of the antibody–lipid hapten reaction is

$$A + H \underset{k_{-1}}{\overset{k_1}{\rightleftharpoons}} AH \underset{-H}{\overset{+H}{\overset{k_2}{\rightleftharpoons}}} AH_2 \quad (k_{-2})$$

where A and H represent antibody and lipid hapten, respectively, and all k_i are rate constants.

Experimentally, TIRFM can only distinguish between free and bound antibody, namely, A and the sum of AH and AH_2. Therefore, the initial rates of association in all curves of Figure 5 can be approximated by

$$\left(\frac{d[AH]}{dt}\right)_{t=0} = k_1[A][H] \quad (2)$$

where [A] and [H] are the initial concentrations of antibody and hapten, respectively. The association rate constants were calculated according to eq 2, and the results are listed in Table IV. A small lag phase which reflects the time needed for complete mixing and diffusion through unstirred layers of the solution near the membrane surface was subtracted. The association rate constants agree well for all three measurements and yield an average association rate constant of 1.2×10^3 M^{-1} s^{-1}. For a comparison, association rates were also measured with LUVs and analyzed in a similar manner (no lag phase was observed). These constants were in good agreement with those obtained by TIRFM and were also included in Table IV. The observation that our initial association rates are proportional to the binding site concentration in the membrane indicates that the antibody–lipid hapten reaction is not diffusion-controlled (Berg & Purcell, 1977). Similar conclusions were reached on the binding of a monoclonal antibody (IgE) to its receptor on basophilic cells (Wank et al., 1983). Association kinetics of IgGs with other membrane-associated haptens (Petrossian & Owicki, 1984) are faster than those reported in the present work, but again these rates were much smaller than the association rates of the soluble haptens [data not shown; for a review on binding kinetics of soluble haptens to antibodies see Pecht and Lancet (1977)].

Table IV: Association Rate Constants (k_1) of Antibody–Lipid Hapten Binding in Supported Planar Membranes and Large Unilamellar Vesicles

lipid hapten in membrane (mol %)	total lipid concn (μM)	total antibody concn (nM)	$(d[AH]/dt)_{t=0}$ $\times 10^{12}$ (M s^{-1})	$k_1 \times 10^{-3}$ (M^{-1} s^{-1})
Supported Planar Bilayers				
1.0	1.8	75	1.5	1.1
1.0	1.8	150	3.2	1.2
5.0	1.8	150	17	1.3
Large Unilamellar Vesicles				
1.0	230	10	21	0.91
1.0	153	10	20	1.4
5.0	66.5	10	67	2.0
5.0	49.2	10	59	2.4
5.0	32.8	10	42	2.5

The dissociation kinetics (Figure 6) are more difficult to interpret. The generation of free antibody must depend on all four rate constants of the above scheme. Assuming a pseudo-first-order rate law of dissociation, we estimated the overall dissociation rate constant to be of the order of 10^{-4} s^{-1}. In support of kinetic interpretation the ratio of the association and dissociation rate constants agrees remarkably well with the apparent equilibrium binding constants. The problem of antibody dissociation from haptens in model membranes has been discussed in more detail by Parce et al. (1979). Interestingly, their overall dissociation reaction followed a time course very similar to the one reported here.

Taken together, our results demonstrate that the method of TIRFM combined with the SPB technology is a powerful method to examine protein binding to membranes. As is easily seen from a comparison of Figures 3 and 4, this new technique is superior to the vesicle binding assay in which light scattering causes a high background signal. It also eliminates artifacts sometimes observed with highly curved model membranes and vesicle cross-linking. "Solid-phase assays" are currently very popular for studying the binding of large proteins to membrane-associated receptors. In these assays, the ligand is "coated" onto plastic or other supports. For several reasons, these assays can only give qualitative answers (Engel, 1984) and are difficult to compare with each other. Such complications are not expected with TIRFM on SPBs. Furthermore, it should be possible to follow the aggregation behavior of bound ligands and their receptors by lateral diffusion measurements and fluorescence microscopy [see Tamm (1988)]. From an inspection of Table IV, it may be concluded that even at low binding site concentrations binding constants as low as 10^4 M^{-1} should still be measurable by TIRFM.

ACKNOWLEDGMENTS

We thank Ingrid Bartoldus for expert technical assistance.

Registry No. DMPC, 18194-24-6.

REFERENCES

Ames, B. N., & Dubin, D. T. (1960) *J. Biol. Chem. 235*, 769–775.

Axelrod, D. (1983) *J. Membr. Biol. 75*, 1–10.

Axelrod, D., Burghardt, T. P., & Thompson, N. L. (1984) *Annu. Rev. Biophys. Bioeng. 13*, 247–268.

Balakrishnan, K., Mehdi, S. Q., & McConnell, H. M. (1982) *J. Biol. Chem. 257*, 6434–6439.

Berg, H. C., & Purcell, E. M. (1977) *Biophys. J. 20*, 193–219.

Coleman, P. M., Deisenhofer, J., & Huber, R. (1976) *J. Mol. Biol. 100*, 257–282.

Eisen, H. N., & Siskind, G. W. (1964) *Biochemistry 3*, 996–1008.

Engel, J. (1984) *Ciba Foundation Symposia 108*, 108–111.

Harrick, N. J. (1967) in *Internal Reflection Spectroscopy*, Harrick Scientific Corp., New York.

Hirschfeld, T. (1965) *Can. Spectrosc. 10*, 128.

Jacobson, K., Elson, E., Koppel, D., & Webb, W. (1983) *Fed. Proc. Fed. Am. Soc. Exp. Biol. 42*, 72–79.

Karush, F. (1978) *Comp. Immunol. 5*, 85–116.

Kinsky, S. C., & Nicoletti, R. A. (1977) *Annu. Rev. Biochem. 46*, 49–67.

Klausner, R. D., van Renswoude, J., Blumenthal, R., & Rivnay, B. (1984) in *Molecular and Chemical Characterization of Membrane Receptors* (Venter, J. C., & Harrison, L. C., Eds.) pp 209–239, Alan R. Liss, New York.

Klotz, I. M. (1982) *Science 217*, 1247–1249.

Kronick, M. N., & Little, W. A. (1975) *J. Immunol. Methods 8*, 235–240.

Kuchinka, E., & Seelig, J. (1989) *Biochemistry 28*, 4216–4221.

Lowry, O. H., Rosebrough, N. J., Farr, A. L., & Randall, R. J. (1951) *J. Biol. Chem. 87*, 848–852.

McConnell, H. M., Watts, T. H., Weiss, R. M., & Brian, A. A. (1986) *Biochim. Biophys. Acta 864*, 95–106.

Metzger, H., Alcoraz, G., Hohman, R., Kinet, J. P., Pribluda, V., & Quarto, R. (1986) *Annu. Rev. Immunol. 4*, 419–470.

Montal, M., Darszon, A., & Schindler, H. (1981) *Q. Rev. Biophys. 14*, 1–79.

Parce, J. W., Schwarz, M. A., Owicki, J. C., & McConnell, H. M. (1979) *J. Phys. Chem. 83*, 3414–3417.

Pecht, I., & Lancet, D. (1977) in *Chemical Relaxation in Molecular Biology* (Pecht, I., & Rigler, R., Eds.) pp 306–338, Springer, New York.

Petrossian, A., & Owicki, J. C. (1984) *Biochim. Biophys. Acta 776*, 217–227.

Sadegh-Nasseri, S., & McConnell, H. M. (1989) *Nature 337*, 274–276.

Schlessinger, J. (1988) *Biochemistry 27*, 3119–3123.

Schneider, G., Knoll, W., Sackmann, E., & Joosten, J. G. H. (1986) *Europhys. Lett. 1*, 449–454.

Stankowski, S. (1983) *Biochim. Biophys. Acta 735*, 352–360.

Sui, S., Urumow, T., & Sackmann, E. (1988) *Biochemistry 27*, 7463–7469.

Tamm, L. K. (1988) *Biochemistry 27*, 1450–1457.

Tamm, L. K., & McConnell, H. M. (1985) *Biophys. J. 47*, 105–113.

Tamm, L. K., & Bartoldus, I. (1988) *Biochemistry 27*, 7453–7458.

Tamm, L. K., Tomich, J. M., & Saier, M. H., Jr. (1989) *J. Biol. Chem. 264*, 2587–2592.

Thompson, N. L., & Axelrod, D. (1983) *Biophys. J. 43*, 103–114.

Wank, S. A., DeLisi, C., & Metzger, H. (1983) *Biochemistry 22*, 954–959.

Watts, T. H., Brian, A. A., Kappler, J. W., Marrack, P., & McConnell, H. M. (1984) *Proc. Natl. Acad. Sci. U.S.A. 81*, 7564–7568.

Watts, T. H., Gaub, H. E., & McConnell, H. M. (1986) *Nature 320*, 179–181.

Weis, R. M., Balakrishnan, K., Smith, B. A., & McConnell, H. M. (1982) *J. Biol. Chem. 237*, 6440–6445.

White, S. H., & King, G. I. (1985) *Proc. Natl. Acad. Sci. U.S.A 82*, 6532–6536.

Wright, L. L., Palmer, A. G., & Thompson, N. L. (1988) *Biophys. J. 54*, 463–470.